

PUBLISHED VERSION

Guo, Xin-Heng; Thomas, Anthony William; Williams, Anthony Gordon
[Heavy quark distribution functions in heavy baryons](#) Physical Review D, 2001;
64(9):096004

© 2001 American Physical Society

<http://link.aps.org/doi/10.1103/PhysRevD.64.096004>

PERMISSIONS

<http://publish.aps.org/authors/transfer-of-copyright-agreement>

“The author(s), and in the case of a Work Made For Hire, as defined in the U.S. Copyright Act, 17 U.S.C.

§101, the employer named [below], shall have the following rights (the “Author Rights”):

[...]

3. The right to use all or part of the Article, including the APS-prepared version without revision or modification, on the author(s)’ web home page or employer’s website and to make copies of all or part of the Article, including the APS-prepared version without revision or modification, for the author(s)’ and/or the employer’s use for educational or research purposes.”

5th April 2013

<http://hdl.handle.net/2440/11164>

Heavy Quark Distribution Functions in Heavy Baryons

X.-H. Guo, A.W. Thomas and A.G. Williams

Department of Physics and Mathematical Physics,
and Special Research Center for the Subatomic Structure of Matter,
Adelaide University, SA 5005, Australia

e-mail: xhguo@physics.adelaide.edu.au, athomas@physics.adelaide.edu.au,
awilliam@physics.adelaide.edu.au

Abstract

Using the Bethe-Salpeter (B-S) equations for heavy baryons Λ_Q , Σ_Q , Ξ_Q and Ω_Q ($Q = b$ or c), which were established in previous work, we calculate the heavy quark distribution functions in these baryons. The numerical results indicate that these distribution functions have an obvious peak at some fraction, α_0 , of the baryon's light-cone "plus" momentum component carried by the heavy quark, and that as m_Q becomes heavier this peak becomes sharper and closer to 1. The dependence of the distribution functions on various input parameters in the B-S model is also discussed. The results are seen to be qualitatively similar to an existing phenomenological model.

PACS Numbers: 11.10.St, 14.20.Mr, 14.20.Lq

I. Introduction

A significant amount of experimental data have been accumulated on lepton nucleon deep inelastic scattering processes. From these data one can extract information on the parton distribution functions in the nucleon, which describe its nonperturbative hadronic structure. In comparison with the nucleon, much less is known about the parton distribution functions in other baryons such as Λ , Λ_c , and Λ_b . This is because it is impossible to produce targets of these short lived baryons suitable for experiments. Although the parton distribution functions in these baryons cannot be studied through deep inelastic scattering processes, it is still possible to obtain information on their parton distribution functions by measuring the fragmentation of quarks to baryons or the decays of these baryons. In fact, the parton distribution functions in Λ , Σ and Δ have been calculated in the MIT bag model dressed by mesons [1]. In this paper, we will study the heavy quark distribution functions in heavy baryons.

The dynamics inside a heavy hadron is simplified by the fact that the light degrees of freedom in a heavy hadron are blind to the flavor and spin quantum numbers of the heavy quark when its mass is much bigger than the QCD scale [2]. This makes heavy flavor physics a good area for studying nonperturbative QCD interactions. In fact, with more measurements on heavy baryons becoming available [3, 4, 5, 6], theoretical study of the structure of heavy baryons is becoming increasingly important.

The parton distribution functions are scale-dependent, and their evolution in the perturbative region is described by the famous Dokshitzer- Gribov-Lipatov-Altarelli-Parisi (DGLAP) equations [7]. However, to determine the parton distribution functions at some low energy scale (the boundary condition for DGLAP), one needs to apply either lattice QCD [8] or nonperturbative effective models. In the heavy quark limit, the light degrees of freedom in a heavy baryon have good quantum

numbers which can be used to classify heavy baryons. Based on this fact, in a previous work we took the heavy baryon to be composed of a heavy quark and a light diquark. With this picture, we established the B-S equations for the heavy baryons Λ_Q and ω_Q (where ω represents Σ , Ξ , or Ω), and solved these equations numerically by assuming that their kernel contains a scalar confinement term and a one-gluon-exchange term [9]. It is the purpose of the present paper to calculate the heavy quark distribution functions in these heavy baryons in our B-S formalism.

In Λ_Q and ω_Q we have 0^+ and 1^+ diquarks, respectively. Since in the heavy quark limit the internal dynamics of a heavy baryon are described by the light degrees of freedom, we expect that the heavy quark distribution functions in ω_Q and ω_Q^* should be the same. Furthermore, the differences among the heavy quark distribution functions in Σ_Q , Ξ_Q , and Ω_Q should be caused by $SU(3)$ flavor breaking effects.

The remainder of this paper is organized as follows. In Section II we derive the formulas for the heavy quark distribution functions in various heavy baryons in the B-S formalism. In Section III we present numerical results for these distribution functions and discuss their dependence on the parameters of the model. We also compare our results with the distribution functions of Guo and Kroll [10]. Finally, we give a summary and some suggestions for future work in Section IV.

II. Formalism for the heavy quark distribution functions in Λ_Q , Σ_Q , Ξ_Q and Ω_Q

Based on the picture that a heavy baryon is composed of a heavy quark and a light diquark, it was shown that the B-S equation for Λ_Q is [9]

$$\chi_P(p) = S_F(\lambda_1 P + p) \int \frac{d^4 q}{(2\pi)^4} G(P, p, q) \chi_P(q) S_D(-\lambda_2 P + p), \quad (1)$$

where $\chi_P(p)$ is the B-S wave function in momentum space, $G(P, p, q)$ is the kernel, S_F and S_D are the propagators of the heavy quark and light scalar diquark, respectively,

with $\lambda_1 = \frac{m_Q}{m_Q+m_D}$ and $\lambda_2 = \frac{m_D}{m_Q+m_D}$ (m_Q and m_D are the masses of the heavy quark and the light diquark, respectively), P is the momentum of Λ_Q , and p is the relative momentum of the two constituents.

Similarly, the B-S equation for ω_Q takes the form

$$\chi_P^\mu(p) = S_F(\lambda_1 P + p) \int \frac{d^4 q}{(2\pi)^4} G_{\rho\nu}(P, p, q) \chi_P^\nu(q) S_D^{\mu\rho}(-\lambda_2 P + p), \quad (2)$$

where $G_{\rho\nu}(P, p, q)$ is the kernel and $S_D^{\mu\rho}$ is the propagator of the 1^+ diquark.

In the heavy quark limit

$$\chi_{0P}(p) = \phi_{0P}(p) u_{\Lambda_Q}(v, s), \quad (3)$$

where $\phi_{0P}(p)$ is a scalar function, and $u_{\Lambda_Q}(v, s)$ is the Dirac spinor for Λ_Q with helicity s and velocity v .

For ω_Q there are three scalar functions, A, C and D , in the B-S wave function

$$\chi_P^\mu = AB^\mu(v) + Cv^\mu p_{t\nu} B^\nu(v) + Dp_t^\mu p_{t\nu} B^\nu(v), \quad (4)$$

where $B_\mu(v) = \frac{1}{\sqrt{3}}(\gamma_\mu + v_\mu)\gamma_5 u(v)$, and $p_t \equiv p - (v \cdot p)v$. $B_\mu(v)$ satisfies the constraints $\not{p} B_\mu(v) = B_\mu(v)$ and $v^\mu B_\mu(v) = 0$.

The B-S equations have been solved numerically in the covariant instantaneous approximation, assuming the kernels contain a scalar confinement term, \tilde{V}_1 , and a one-gluon-exchange term, \tilde{V}_2 , with the following form

$$\begin{aligned} \tilde{V}_1 &= \frac{8\pi\kappa}{[(p_t - q_t)^2 + \mu^2]^2} - (2\pi)^3 \delta^3(p_t - q_t) \int \frac{d^3 k}{(2\pi)^3} \frac{8\pi\kappa}{(k^2 + \mu^2)^2}, \\ \tilde{V}_2 &= -\frac{16\pi}{3} \frac{\alpha_s^{(\text{eff})2} Q_0^2}{[(p_t - q_t)^2 + \mu^2][(p_t - q_t)^2 + Q_0^2]}, \end{aligned} \quad (5)$$

where κ and $\alpha_s^{(\text{eff})}$ are coupling parameters related to scalar confinement and one-gluon-exchange, respectively, where Q_0^2 is a parameter associated with the gluon-diquark vertex, and where the parameter μ is introduced to avoid the infra-red divergence in numerical calculations, with the limit $\mu \rightarrow 0$ being taken at the end of the calculation.

The twist-2 heavy quark distribution function in $A^+ = 0$ gauge is defined as [11, 12]

$$Q(\alpha) = \sqrt{2}P^+ \int \frac{dx^-}{2\pi} e^{-i\alpha P^+ x^-} \langle B | T \bar{\psi}_Q(x^-) \gamma^+ \psi_Q(0) | B \rangle, \quad (6)$$

where ψ_Q is the field operator of the heavy quark Q , $P^+ = \frac{1}{\sqrt{2}}(P^0 + P^3)$, $\gamma^+ = \frac{1}{\sqrt{2}}(\gamma^0 + \gamma^3)$, $\psi_Q(x^-)$ denotes $\psi_Q(x)$ at $x^+ = \mathbf{x}_\perp = 0$, and $|B\rangle$ represents the heavy baryon state with the normalization $\langle B, \mathbf{P}, \lambda | B, \mathbf{P}', \lambda' \rangle = (2\pi)^3 P_0 / m_B \delta_{\lambda, \lambda'} \delta^3(\mathbf{P} - \mathbf{P}')$ (we have chosen the normalization convention $\bar{u}_B u_B = 1$).

We define the two-point function

$$M_{\beta\alpha}(P, k) = \int d^4x e^{-ikx} \langle B | T \bar{\psi}_{Q\alpha}(x) \psi_{Q\beta}(0) | B \rangle \quad (7)$$

and then the heavy quark distribution function can be expressed as

$$Q(\alpha) = \int \frac{d^4k}{(2\pi)^4} \sqrt{2}P^+ \delta(k^+ - \alpha P^+) \text{Tr}[\gamma^+ M(P, k)]. \quad (8)$$

The parameter α in Eqs. (6,8) corresponds to the fraction of the heavy baryon's light-cone momentum component, P^+ , carried by the heavy quark, Q . When it is in the range $0 \leq \alpha \leq 1$, $Q(\alpha)$ measures the probability to find the heavy quark with the “plus” momentum fraction α . In principle, in a heavy baryon there is a possibility to find a heavy antiquark, which is generated from the QCD vacuum. However, since we are considering heavy quarks with masses much larger than the QCD scale Λ_{QCD} , it is very difficult to produce them from the QCD vacuum. Therefore, we neglect the heavy antiquark distribution functions. In other words, the valence heavy quark distribution function is the same as the heavy quark distribution function, $Q(\alpha)$. Since there is only one heavy quark in a heavy baryon we have the following normalization condition for $Q(\alpha)$:

$$\int d\alpha Q(\alpha) = 1. \quad (9)$$

The two-point function $M(P, k)$ can be evaluated in our B-S framework. After some algebra we obtain for Λ_Q in the heavy quark limit the result

$$M_{\beta\alpha}^{\Lambda_Q}(P, k) = (\bar{u}_{\Lambda_Q})_\alpha [\phi_{0P}(k - \lambda_1 P)]^2 S_D^{-1}(P - k) (u_{\Lambda_Q})_\beta. \quad (10)$$

The propagator of the light scalar diquark has the form

$$S_D = \frac{i}{p_l^2 - W_p^2 + i\epsilon}, \quad (11)$$

where $p_l \equiv v \cdot p - \lambda_2 m_{\Lambda_Q}$ and $W_p \equiv \sqrt{p_t^2 + m_D^2}$.

The propagator of the heavy quark in the heavy quark limit has the form

$$S_F = \frac{i(1 + \psi)}{2(p_l + E_0 + m_D + i\epsilon)}, \quad (12)$$

where E_0 is the binding energy in the heavy quark limit.

We choose to work in the rest frame of Λ_Q , in which we have $k^0 + k^3 = \alpha m_{\Lambda_Q}$ (m_{Λ_Q} is the mass of Λ_Q) from the $\delta(k^+ - \alpha P^+)$ constraint in Eq. (8). Hence we find

$$S_D^{-1} = -i[-|\mathbf{k}_\perp|^2 + 2(1 - \alpha)m_{\Lambda_Q}k^3 + (1 - \alpha)^2m_{\Lambda_Q}^2 - m_D^2]. \quad (13)$$

The B-S wave function, $\phi_{0P}(p)$, can be expressed in terms of $\tilde{\phi}_{0P}(q_t) \equiv \int \frac{dp_l}{2\pi} \phi_{0P}(p)$ as [9]:

$$\phi_{0P}(p) = \frac{i}{(p_l + E_0 + m_D + i\epsilon)(p_l^2 - W_p^2 + i\epsilon)} \int \frac{d^3q_t}{(2\pi)^3} (\tilde{V}_1 + 2p_l\tilde{V}_2) \tilde{\phi}_{0P}(q_t). \quad (14)$$

The constraint $\delta(k^+ - \alpha P^+)$ leads to $p_l = -k^3 + (\alpha - 1)m_{\Lambda_Q}$, and $|p_t|^2 = |\mathbf{k}_\perp|^2$. Substituting Eqs. (10,14) into Eq. (8), we integrate out k^0 with the aid of $\delta(k^+ - \alpha P^+)$. Furthermore, the component k^3 can also be integrated out by choosing the appropriate contour. Then we arrive at the following result:

$$\begin{aligned} Q^{\Lambda_Q}(\alpha) &= \frac{1}{2\sqrt{2}\pi(1 - \alpha)} \int \frac{d^2\mathbf{k}_\perp}{(2\pi)^2} \frac{1}{[E_0 + m_D + \frac{1}{2}(\alpha - 1)m_{\Lambda_Q} + \frac{1}{2(\alpha - 1)m_{\Lambda_Q}}(|\mathbf{k}_\perp|^2 + m_D^2)]^2} \\ &\quad \left\{ \int \frac{d^3q_t}{(2\pi)^3} \left[\tilde{V}_1(p_t - q_t) + \left((\alpha - 1)m_{\Lambda_Q} + \frac{1}{(\alpha - 1)m_{\Lambda_Q}}(|\mathbf{k}_\perp|^2 + m_D^2) \right) \right. \right. \\ &\quad \left. \left. \tilde{V}_2(p_t - q_t) \right] \tilde{\phi}_{0P}(q_t) \right\}^2, \end{aligned} \quad (15)$$

where $|p_t|^2 = |\mathbf{k}_\perp|^2 + (k_{\text{pole}}^3)^2$ and where $k_{\text{pole}}^3 = \frac{1}{2(\alpha - 1)m_{\Lambda_Q}}[(\alpha - 1)^2m_{\Lambda_Q}^2 - |\mathbf{k}_\perp|^2 - m_D^2]$.

Substituting \tilde{V}_1 and \tilde{V}_2 in Eq. (5) into Eq. (15) and integrating out the angular coordinates we finally obtain

$$Q^{\Lambda_Q}(\alpha) = \frac{1}{2\sqrt{2}\pi(1 - \alpha)} \int \frac{|\mathbf{k}_\perp| d|\mathbf{k}_\perp|}{2\pi} \frac{1}{[E_0 + m_D + \frac{1}{2}(\alpha - 1)m_{\Lambda_Q} + \frac{1}{2(\alpha - 1)m_{\Lambda_Q}}(|\mathbf{k}_\perp|^2 + m_D^2)]^2}$$

$$\begin{aligned}
& \left(\int \frac{q_t^2 dq_t}{4\pi^2} \left\{ \frac{16\pi\kappa}{(p_t^2 + q_t^2 + \mu^2)^2 - 4p_t^2 q_t^2} [\tilde{\phi}_{0P}(q_t) - \tilde{\phi}_{0P}(p_t)] \right. \right. \\
& + \frac{16\pi\alpha_s^{\text{eff}2} Q_0^2}{3(Q_0^2 - \mu^2)} \left[(\alpha - 1)m_{\Lambda_Q} + \frac{1}{(\alpha - 1)m_{\Lambda_Q}} (|\mathbf{k}_\perp|^2 + m_D^2) \right] \\
& \left. \left. \times \frac{1}{2|p_t||q_t|} \left[\ln \frac{(|p_t| + |q_t|)^2 + \mu^2}{(|p_t| - |q_t|)^2 + \mu^2} - \ln \frac{(|p_t| + |q_t|)^2 + Q_0^2}{(|p_t| - |q_t|)^2 + Q_0^2} \right] \tilde{\phi}_{0P}(q_t) \right\} \right)^2, \quad (16)
\end{aligned}$$

where

$$|p_t| = \frac{1}{2(1 - \alpha)m_{\Lambda_Q}} \sqrt{[(\alpha - 1)^2 m_{\Lambda_Q}^2 - |\mathbf{k}_\perp|^2 - m_D^2]^2 + 4(\alpha - 1)^2 |\mathbf{k}_\perp|^2 m_{\Lambda_Q}^2}. \quad (17)$$

In deriving Eq. (16) we have used the following equations to reduce the three dimensional integrations to one dimensional integrations

$$\int \frac{d^3 q_t}{(2\pi)^3} \frac{\rho(q_t^2)}{[(p_t - q_t)^2 + \mu^2]^2} = \int \frac{q_t^2 dq_t}{4\pi^2} \frac{2\rho(q_t^2)}{(p_t^2 + q_t^2 + \mu^2)^2 - 4p_t^2 q_t^2}, \quad (18)$$

and

$$\int \frac{d^3 q_t}{(2\pi)^3} \frac{\rho(q_t^2)}{(p_t - q_t)^2 + \delta^2} = \int \frac{q_t^2 dq_t}{4\pi^2} \frac{\rho(q_t^2)}{2|p_t||q_t|} \ln \frac{(|p_t| + |q_t|)^2 + \delta^2}{(|p_t| - |q_t|)^2 + \delta^2}, \quad (19)$$

where $\rho(q_t^2)$ is some arbitrary scalar function of q_t^2 .

Now we turn to ω_Q . The two-point function $M(P, k)$ in this case can be derived in a similar way and the result is

$$M_{\beta\alpha}^{\omega_Q}(P, k) = \bar{\chi}_\alpha^\mu(k - \lambda_1 P) S_{D\mu\nu}^{-1}(P - k) \chi_\beta^\nu(k - \lambda_1 P). \quad (20)$$

Substituting the B-S equation (2) into Eq. (20), using Eqs. (4) and (12), and working in the covariant instantaneous approximation, $p_l = q_l$ (which ensures that the B-S equation is still covariant after this approximation), we have

$$\begin{aligned}
\text{Tr}[\gamma^+ M^{\omega_Q}(P, k)] &= \frac{1}{p_l + E_0 + m_D + i\epsilon} [A\bar{B}^\mu + Cv^\mu p_t \cdot \bar{B} + Dp_t^\mu p_t \cdot \bar{B}] \gamma^+ \\
& \int \frac{d^3 q_t}{(2\pi)^3} \left\{ B_\mu \left[\tilde{A}(\tilde{V}_1 + 2p_l \tilde{V}_2) - \tilde{C} \frac{(p_t \cdot q_t)^2 - p_t^2 q_t^2}{2p_t^2} \tilde{V}_2 \right. \right. \\
& \left. \left. + \tilde{D} \frac{(p_t \cdot q_t)^2 - p_t^2 q_t^2}{2p_t^2} (\tilde{V}_1 + 2p_l \tilde{V}_2) \right] \right. \\
& + v_\mu p_t \cdot B \left[-\tilde{A}\tilde{V}_2 - \frac{p_t \cdot q_t}{p_t^2} \tilde{C}\tilde{V}_1 + \tilde{D} \frac{(p_t \cdot q_t)^2}{p_t^2} \tilde{V}_2 \right] \\
& \left. + p_{t\mu} p_t \cdot B \frac{3(p_t \cdot q_t)^2 - p_t^2 q_t^2}{2p_t^4} [-\tilde{C}\tilde{V}_2 + \tilde{D}(\tilde{V}_1 + 2p_l \tilde{V}_2)] \right\}. \quad (21)
\end{aligned}$$

As for Λ_Q , the B-S wave functions $A(p_l, p_t^2)$, $C(p_l, p_t^2)$ and $D(p_l, p_t^2)$ are related to $\tilde{A}(p_t^2)$, $\tilde{C}(p_t^2)$ and $\tilde{D}(p_t^2)$ through the following equations [9]:

$$A(p_l, p_t^2) = \frac{-i}{(p_l + E_0 + m_D + i\epsilon)(p_t^2 - W_p^2 + i\epsilon)} \int \frac{d^3 q_t}{(2\pi)^3} \left\{ \tilde{A}(q_t^2)(\tilde{V}_1 + 2p_l \tilde{V}_2) - \tilde{C}(q_t^2) \frac{(p_t \cdot q_t)^2 - p_t^2 q_t^2}{2p_t^2} \tilde{V}_2 + \tilde{D}(q_t^2) \frac{(p_t \cdot q_t)^2 - p_t^2 q_t^2}{2p_t^2} (\tilde{V}_1 + 2p_l \tilde{V}_2) \right\}, \quad (22)$$

$$C(p_l, p_t^2) = \frac{-i}{m_D^2(p_l + E_0 + m_D + i\epsilon)(p_t^2 - W_p^2 + i\epsilon)} \int \frac{d^3 q_t}{(2\pi)^3} \left\{ -\tilde{A}(q_t^2)[p_l \tilde{V}_1 + (p_t^2 + m_D^2)\tilde{V}_2] - \tilde{C}(q_t^2) \left[(p_t^2 - m_D^2) \frac{p_t \cdot q_t}{p_t^2} \tilde{V}_1 + p_l \frac{(p_t \cdot q_t)^2}{p_t^2} \tilde{V}_2 \right] + \tilde{D}(q_t^2) \frac{(p_t \cdot q_t)^2}{p_t^2} [p_l \tilde{V}_1 + (p_t^2 + m_D^2)\tilde{V}_2] \right\}, \quad (23)$$

$$D(p_l, p_t^2) = \frac{i}{m_D^2(p_l + E_0 + m_D + i\epsilon)(p_t^2 - W_p^2 + i\epsilon)} \int \frac{d^3 q_t}{(2\pi)^3} \left\{ \tilde{A}(q_t^2)(\tilde{V}_1 + p_l \tilde{V}_2) + \tilde{C}(q_t^2) \left[\frac{p_t \cdot q_t}{p_t^2} p_l \tilde{V}_1 + \frac{m_D^2(3(p_t \cdot q_t)^2 - p_t^2 q_t^2) + 2p_t^2(p_t \cdot q_t)^2}{2p_t^4} \tilde{V}_2 \right] + \tilde{D}(q_t^2) \left[-\frac{m_D^2(3(p_t \cdot q_t)^2 - p_t^2 q_t^2) + 2p_t^2(p_t \cdot q_t)^2}{2p_t^4} (\tilde{V}_1 + 2p_l \tilde{V}_2) + \frac{(p_t \cdot q_t)^2}{p_t^2} p_l \tilde{V}_2 \right] \right\}, \quad (24)$$

and $\tilde{A}(p_t^2)$, $\tilde{C}(p_t^2)$ and $\tilde{D}(p_t^2)$ obey the following three coupled integral equations

$$\tilde{A}(p_t^2) = \frac{-1}{2W_p(E_0 + m_D - W_p)} \int \frac{d^3 q_t}{(2\pi)^3} \left\{ \tilde{A}(q_t^2)(\tilde{V}_1 - 2W_p \tilde{V}_2) - \tilde{C}(q_t^2) \frac{(p_t \cdot q_t)^2 - p_t^2 q_t^2}{2p_t^2} \tilde{V}_2 + \tilde{D}(q_t^2) \frac{(p_t \cdot q_t)^2 - p_t^2 q_t^2}{2p_t^2} (\tilde{V}_1 - 2W_p \tilde{V}_2) \right\}, \quad (25)$$

$$\tilde{C}(p_t^2) = \frac{-1}{2m_D^2 W_p(E_0 + m_D - W_p)} \int \frac{d^3 q_t}{(2\pi)^3} \left\{ \tilde{A}(q_t^2)[W_p \tilde{V}_1 - ((E_0 + m_D)W_p + m_D^2)\tilde{V}_2] + \tilde{C}(q_t^2) \left[-\frac{p_t \cdot q_t}{p_t^2} ((E_0 + m_D)W_p - m_D^2)\tilde{V}_1 + W_p \frac{(p_t \cdot q_t)^2}{p_t^2} \tilde{V}_2 \right] + \tilde{D}(q_t^2) \frac{(p_t \cdot q_t)^2}{p_t^2} [-W_p \tilde{V}_1 + ((E_0 + m_D)W_p + m_D^2)\tilde{V}_2] \right\}, \quad (26)$$

$$\begin{aligned}
\tilde{D}(p_t^2) &= \frac{1}{2m_D^2 W_p (E_0 + m_D - W_p)} \int \frac{d^3 q_t}{(2\pi)^3} \left\{ \tilde{A}(q_t^2) (\tilde{V}_1 - W_p \tilde{V}_2) \right. \\
&\quad + \tilde{C}(q_t^2) \left[-\frac{p_t \cdot q_t}{p_t^2} W_p \tilde{V}_1 + \frac{m_D^2 (3(p_t \cdot q_t)^2 - p_t^2 q_t^2) + 2p_t^2 (p_t \cdot q_t)^2}{2p_t^4} \tilde{V}_2 \right] \\
&\quad - \tilde{D}(q_t^2) \left[\frac{m_D^2 (3(p_t \cdot q_t)^2 - p_t^2 q_t^2) + 2p_t^2 (p_t \cdot q_t)^2}{2p_t^4} (\tilde{V}_1 - 2W_p \tilde{V}_2) \right. \\
&\quad \left. \left. + \frac{(p_t \cdot q_t)^2}{p_t^2} W_p \tilde{V}_2 \right] \right\}. \tag{27}
\end{aligned}$$

Once again, we first integrate out k^0 with the help of the constraint $\delta(k^+ - \alpha P^+)$, then we further integrate out k^3 by selecting the proper contour which contains the pole in k^3 . With the aid of Eqs. (22-27), and noticing that $\bar{B}^\mu \gamma^+ B_\mu = -\frac{1}{\sqrt{2}}$ and $p_t \cdot B \gamma^+ p_t \cdot B = \frac{1}{3\sqrt{2}} |\mathbf{k}|^2$, we obtain:

$$\begin{aligned}
Q^{\omega Q}(\alpha) &= \frac{1}{3\sqrt{2}\pi(1-\alpha)} \int \frac{|\mathbf{k}_\perp| d|\mathbf{k}_\perp|}{2\pi} \frac{W_p}{E_0 + m_D - W_p} [-3\tilde{A}(p_t^2) f_1(p_t^2) \\
&\quad + p_t^2 \tilde{C}(p_t^2) f_2(p_t^2) + p_t^2 \tilde{D}(p_t^2) f_3(p_t^2)], \tag{28}
\end{aligned}$$

where $|p_t|$ is given in Eq. (17), and

$$f_1(p_t^2) = \int \frac{d^3 q_t}{(2\pi)^3} \left\{ \tilde{A}(q_t^2) (\tilde{V}_1 - 2W_p \tilde{V}_2) - \frac{1}{3} q_t^2 [-\tilde{C}(q_t^2) \tilde{V}_2 + \tilde{D}(q_t^2) (\tilde{V}_1 - 2W_p \tilde{V}_2)] \right\}, \tag{29}$$

$$f_2(p_t^2) = \int \frac{d^3 q_t}{(2\pi)^3} \left[-\tilde{A}(q_t^2) \tilde{V}_2 + \tilde{C}(q_t^2) \frac{p_t \cdot q_t}{p_t^2} \tilde{V}_1 + \tilde{D}(q_t^2) \frac{(p_t \cdot q_t)^2}{p_t^2} \tilde{V}_2 \right], \tag{30}$$

$$f_3(p_t^2) = \int \frac{d^3 q_t}{(2\pi)^3} \left\{ \tilde{A}(q_t^2) (\tilde{V}_1 - 2W_p \tilde{V}_2) - \frac{(p_t \cdot q_t)^2}{p_t^2} [-\tilde{C}(q_t^2) \tilde{V}_2 + \tilde{D}(q_t^2) (\tilde{V}_1 - 2W_p \tilde{V}_2)] \right\}. \tag{31}$$

So far we have been working with the heavy quark limit, $m_Q \rightarrow \infty$, of the B-S equation, but in Ref. [9] we also considered the $1/m_Q$ corrections to the B-S equation for Λ_Q . To order $1/m_Q$, the heavy quark distribution function in Λ_Q is given by

$$Q^{\Lambda Q}(\alpha) + \Delta Q^{\Lambda Q}(\alpha)$$

where $\Delta Q^{\Lambda Q}(\alpha)$ denotes the $1/m_Q$ corrections. To order $1/m_Q$, two more scalar functions appear in the B-S wave function, which can be related to $\phi_{0P}(p)$ in the

model of Ref. [9]. Consequently, the B-S wave function to order $1/m_Q$ is given by

$$\chi_P(p) = \phi_{0P}(p) \left[1 + \frac{\not{p}_t}{2m_Q} \right] u_{\Lambda_Q}(v, s). \quad (32)$$

With Eq. (32) we can evaluate the two-point function $M_{\beta\alpha}^{\Lambda_Q}(P, k)$ to order $1/m_Q$ from Eq. (10). Note that the scalar diquark propagator in Eq. (11) remains unchanged to order $1/m_Q$. From Eq. (8), after integrating out k^0 and k^3 , we have

$$\begin{aligned} \Delta Q^{\Lambda_Q}(\alpha) &= \frac{1}{2\sqrt{2}\pi(1-\alpha)} \int \frac{|\mathbf{k}_\perp| d|\mathbf{k}_\perp|}{2\pi} \frac{\frac{1}{2}(\alpha-1)m_{\Lambda_Q} - \frac{1}{2(\alpha-1)m_{\Lambda_Q}}(|\mathbf{k}_\perp|^2 + m_D^2)}{[E_0 + m_D + \frac{1}{2}(\alpha-1)m_{\Lambda_Q} + \frac{1}{2(\alpha-1)m_{\Lambda_Q}}(|\mathbf{k}_\perp|^2 + m_D^2)]^2} \\ &\quad \left(\int \frac{q_t^2 dq_t}{4\pi^2} \left\{ \frac{16\pi\kappa}{(p_t^2 + q_t^2 + \mu^2)^2 - 4p_t^2 q_t^2} [\tilde{\phi}_{0P}(q_t) - \tilde{\phi}_{0P}(p_t)] \right. \right. \\ &\quad \left. \left. + \frac{16\pi\alpha_s^{\text{eff}2} Q_0^2}{3(Q_0^2 - \mu^2)} \left[(\alpha-1)m_{\Lambda_Q} + \frac{1}{(\alpha-1)m_{\Lambda_Q}}(|\mathbf{k}_\perp|^2 + m_D^2) \right] \right. \right. \\ &\quad \left. \left. \times \frac{1}{2|p_t||q_t|} \left[\ln \frac{(|p_t| + |q_t|)^2 + \mu^2}{(|p_t| - |q_t|)^2 + \mu^2} - \ln \frac{(|p_t| + |q_t|)^2 + Q_0^2}{(|p_t| - |q_t|)^2 + Q_0^2} \right] \tilde{\phi}_{0P}(q_t) \right\} \right)^2, \end{aligned} \quad (33)$$

where again $|p_t|$ is given in Eq. (17).

The heavy quark distribution functions have been derived at some scale ν_0 , which is of the order of Λ_{QCD} . The QCD running of these functions is controlled by the DGLAP equations. In our numerical calculations we will use the evolution code provided in Ref. [13] to give the heavy quark distribution functions at any higher scale. This will be done to the next-to-leading order. Since the QCD interactions are flavor independent, we can directly apply this code to the cases of heavy quarks. It should be pointed out that the scale ν_0 cannot be determined in our approach. We will treat it as a free parameter and leave it to be determined by the future experimental data.

III. Numerical results

In this section we will give numerical results for the heavy quark distribution

functions based on the formulas presented in Section II. The B-S wave functions for Λ_Q and ω_Q were solved numerically in our previous work by discretizing the integration region $(0, \infty)$ into n pieces (n is chosen to be sufficiently large and we use n -point Gauss quadrature rule to evaluate the integrals) and solving the eigenvalue equation with the kernel \tilde{V}_1 and \tilde{V}_2 in Eq. (5) in the covariant instantaneous approximation [9]. The normalization constants of these B-S wave functions are determined by the normalization of Isgur-Wise functions at the zero-recoil point. Substituting these numerical solutions into Eqs. (16,28,33), we can obtain numerical results for the heavy quark distribution functions in Λ_Q and ω_Q .

In our model we have several parameters, i.e., $\alpha_s^{(\text{eff})}$, κ , Q_0^2 , m_D and E_0 . The parameter Q_0^2 is chosen to be 3.2GeV^2 from the data for the electromagnetic form factor of the proton [9, 14]. The parameters $\alpha_s^{(\text{eff})}$ and κ are related to each other when we solve the eigenvalue equations with fixed eigenvalues [9]. The parameter κ is of the order $\Lambda_{\text{QCD}}\kappa'$ where κ' is around 0.2GeV^2 from the potential model [15, 16]. Thus we let κ vary in the region between 0.02GeV^3 and 0.1GeV^3 [9]. The parameters m_D and E_0 are constrained by the relation $m_D + E_0 + \frac{1}{m_Q}E_1 = m_{\Lambda_Q} - m_Q$ for Λ_Q (to order $1/m_Q$) and $m_D + E_0 = m_{\omega_Q} - m_Q$ for ω_Q ($m_Q \rightarrow \infty$). From the heavy quark effective theory, $m_D + E_0$ and E_1 are independent of the flavor of the heavy quark. It was shown [9] that the value of E_1 (which is of the order $\Lambda_{\text{QCD}}E_0$) influences the numerical results only slightly. In our numerical calculations we use $m_b = 5.02\text{GeV}$ and $m_c = 1.58\text{GeV}$ which led to consistent predictions with experiments from the B-S equation solutions in the meson case [16]. Consequently we have $m_D + E_0 + \frac{1}{m_b}E_1 = 0.62\text{GeV}$ for Λ_Q (where we have neglected $1/m_b^2$ corrections), and $m_D + E_0 = 0.88\text{GeV}$ for Σ_Q , 1.07GeV for Ξ_Q , 1.12GeV for Ω_Q in the heavy quark limit. The parameter m_D cannot be determined and hence we let it vary within some reasonable range. For Λ_Q , we choose m_D to be in the range $0.65\text{GeV} \sim 0.75\text{GeV}$ [9, 17]. The axial-vector diquark mass is chosen to vary from 0.9GeV to

1GeV for Σ_Q , from 1.1GeV to 1.2GeV for Ξ_Q , and from 1.15GeV to 1.25GeV for Ω_Q [9]. With these choices for m_D , the binding energy E_0 is negative and varies from around -30MeV to -130MeV.

With these parameters, from Eqs. (16,28,33), we obtain numerical results for the heavy quark distribution functions in Λ_Q and ω_Q . These results are shown in Figs.1 to 5. Figs.1(a), 2(a), 3(a), 4(a) and 5(a) show the dependence on κ for a typical m_D , and the dependence on m_D for $\kappa=0.06\text{GeV}^3$. All these results correspond to some low energy scale which is of order several hundred MeV. They are evolved to some higher scale using the DGLAP equations. In Figs.1(b), 2(b), 3(b), 4(b) and 5(b), we show the heavy quark distribution functions at the scale $\nu^2 = 10\text{GeV}^2$, where we have taken the low energy scale ν_0^2 to be 0.25GeV^2 , as an example. From these figures we can see that for different heavy baryons with the same heavy quark flavor the shapes of the heavy quark distribution functions are rather similar. For the heavy quark distribution functions at the hadronic scale, there is an obvious peak at some “plus” momentum fraction carried by the heavy quark, α_0 , and this peak is much sharper for b -baryons than c -baryons. Furthermore, α_0 is much closer to 1 for b -baryons than c -baryons. It can also be seen that QCD evolution makes the amplitudes of the peaks much smaller. However, the distinction between b -quark and c -quark distribution functions is still obvious at high ν^2 . From Figs. 1 to 5 we can also see that with the increase of κ , which represents the strength of confinement, the peaks of the heavy quark distribution functions become lower and their widths bigger. This is because the heavy quark behaves more freely when confinement is weaker.

In Ref. [17] Close and Thomas calculated the u -quark distribution function in the nucleon in the MIT bag model, where numerical results for $\alpha u(\alpha)$ at $\nu^2 = 5 \sim 10\text{GeV}^2$ were shown for various values of the bag radius. It was shown that $\alpha u(\alpha)$ has a maximum value around $0.4 \sim 0.5$ at $\alpha = 0.4 \sim 0.5$. In general their

argument predicts the peak of the valence distribution (for ground state ($L = 0$) baryons) at $(m_H - m_D)/m_H$ (where m_H is the baryon's mass), which is in the range $0.87 \sim 0.88$ for Λ_b and $0.67 \sim 0.72$ for Λ_c , respectively. Clearly these expectations are in excellent agreement with the peak positions at the hadronic scale, ν_0^2 . This statement is also true for ω_Q . We see clearly that with the increase of quark masses, the peak positions of the quark distribution functions move closer to 1 and the peak values become bigger.

In Tables 1,2,3,4 for different heavy baryons with different parameters in our model, we list the values of α_0 , the widths of these peaks, and the total “plus” momentum fraction, f , carried by the heavy quark which is defined as

$$f \equiv \int d\alpha \alpha Q(\alpha). \quad (34)$$

The width is presented by two values of α at which $Q(\alpha)$ is half of its value at the peak, $Q(\alpha_0)$. From these tables we can see the following points: (i) The values of α_0 , f , and the widths depend not only on the light diquark mass m_D but also on κ , and mostly the dependence on κ is more sensitive for c -baryons. (ii) The value of α_0 decreases with the increase of m_D , which is reasonable. (iii) The widths of heavy quark distribution functions for b -baryons are much smaller than those for c -baryons. (iv) For Λ_Q , $1/m_Q$ corrections make α_0 and f bigger. Hence the heavy quark carries more momentum with $1/m_Q$ corrections included. (v) Numerically, in the whole range of parameters we are considering, for Λ_b , α_0 varies from 0.864 to 0.890 (0.870 to 0.890) and f varies from 0.800 to 0.857 (0.810 to 0.860) without (with) $1/m_Q$ corrections, while for Λ_c , α_0 varies from 0.670 to 0.717 (0.690 to 0.760) and f varies from 0.522 to 0.651 (0.585 to 0.672); for Σ_b , α_0 varies from 0.823 to 0.846 and f varies from 0.809 to 0.834, while for Σ_c , α_0 varies from 0.583 to 0.647 and f varies from 0.493 to 0.589; for Ξ_b , α_0 varies from 0.803 to 0.820 and f varies from 0.780 to 0.809, while for Ξ_c , α_0 varies from 0.503 to 0.580 and f varies from 0.412 to 0.520; for Ω_b , α_0 varies from 0.797 to 0.813 and f varies from 0.770 to 0.802,

Table 1: Values of α_0 , widths, and f for Λ_b with and without $1/m_Q$ corrections

$m_D=0.65\text{GeV}$				
$\kappa(\text{GeV}^3)$	0.02 ($O(1)$)	0.02 ($O(1/m_Q)$)	0.10 ($O(1)$)	0.10 ($O(1/m_Q)$)
α_0	0.890	0.890	0.890	0.890
width	0.797 \sim 0.923	0.833 \sim 0.923	0.773 \sim 0.940	0.783 \sim 0.943
f	0.857	0.860	0.822	0.830
$m_D=0.70\text{GeV}$				
$\kappa(\text{GeV}^3)$	0.02 ($O(1)$)	0.02 ($O(1/m_Q)$)	0.10 ($O(1)$)	0.10 ($O(1/m_Q)$)
α_0	0.876	0.878	0.878	0.884
width	0.814 \sim 0.918	0.816 \sim 0.919	0.762 \sim 0.935	0.772 \sim 0.937
f	0.844	0.848	0.811	0.820
$m_D=0.75\text{GeV}$				
$\kappa(\text{GeV}^3)$	0.02 ($O(1)$)	0.02 ($O(1/m_Q)$)	0.10 ($O(1)$)	0.10 ($O(1/m_Q)$)
α_0	0.868	0.870	0.864	0.870
width	0.789 \sim 0.912	0.802 \sim 0.914	0.750 \sim 0.930	0.762 \sim 0.932
f	0.829	0.834	0.800	0.810

while for Ω_c , α_0 varies from 0.533 to 0.580 and f varies from 0.449 to 0.537.

As mentioned in Section II, the heavy quark distribution functions should be normalized according to Eq. (9). For some fixed set of parameters in our model, the B-S wave functions can be completely determined by solving the B-S equations numerically and fixing the normalization of the corresponding Isgur-Wise functions at the zero-recoil point. Hence by checking whether the normalization condition Eq. (9) is satisfied or not we can test whether our model works well. We have performed the integration of $Q(\alpha)$ over α numerically. It is found that for Λ_b and Λ_c , in the whole range of the parameters, $\int d\alpha Q(\alpha)$ is very close to 1 (for Λ_b and Λ_c the deviation from 1 is of order 10^{-4} and $10^{-3} \sim 10^{-2}$, respectively). Furthermore, we find that $1/m_Q$ corrections make $\int d\alpha Q(\alpha)$ even closer to 1. Therefore, our model for $1/m_Q$ corrections works in the right direction. For ω_b and ω_c , although $\int d\alpha Q(\alpha)$ is not as close to 1 as in the case of Λ_Q , the deviation from 1 still happens at order 10^{-2} at most, which is expected to be improved if $1/m_Q$ corrections are also included. Thus the momentum sum rule is satisfied in our model.

Table 2: Values of α_0 , widths, and f for Λ_c with and without $1/m_Q$ corrections

$m_D=0.65\text{GeV}$				
$\kappa(\text{GeV}^3)$	0.02 ($O(1)$)	0.02 ($O(1/m_Q)$)	0.10 ($O(1)$)	0.10 ($O(1/m_Q)$)
α_0	0.717	0.730	0.710	0.760
width	0.580 \sim 0.807	0.600 \sim 0.817	0.443 \sim 0.857	0.510 \sim 0.870
f	0.651	0.672	0.569	0.625
$m_D=0.70\text{GeV}$				
$\kappa(\text{GeV}^3)$	0.02 ($O(1)$)	0.02 ($O(1/m_Q)$)	0.10 ($O(1)$)	0.10 ($O(1/m_Q)$)
α_0	0.697	0.717	0.697	0.730
width	0.537 \sim 0.797	0.563 \sim 0.807	0.417 \sim 0.840	0.487 \sim 0.856
f	0.617	0.645	0.546	0.605
$m_D=0.75\text{GeV}$				
$\kappa(\text{GeV}^3)$	0.02 ($O(1)$)	0.02 ($O(1/m_Q)$)	0.10 ($O(1)$)	0.10 ($O(1/m_Q)$)
α_0	0.670	0.690	0.670	0.713
width	0.500 \sim 0.783	0.530 \sim 0.797	0.387 \sim 0.823	0.550 \sim 0.810
f	0.584	0.618	0.522	0.585

Table 3: Values of α_0 , widths, and f for Σ_b and Σ_c in the heavy quark limit

$m_D=0.90\text{GeV}$				
$\kappa(\text{GeV}^3)$	0.02 (Σ_b)	0.10 (Σ_b)	0.02 (Σ_c)	0.10 (Σ_c)
α_0	0.846	0.843	0.630	0.647
width	0.800 \sim 0.883	0.750 \sim 0.907	0.517 \sim 0.720	0.397 \sim 0.773
f	0.834	0.834	0.589	0.528
$m_D=0.95\text{GeV}$				
$\kappa(\text{GeV}^3)$	0.02 (Σ_b)	0.10 (Σ_b)	0.02 (Σ_c)	0.10 (Σ_c)
α_0	0.840	0.843	0.610	0.600
width	0.780 \sim 0.880	0.733 \sim 0.903	0.470 \sim 0.720	0.463 \sim 0.723
f	0.820	0.813	0.550	0.493
$m_D=1.00\text{GeV}$				
$\kappa(\text{GeV}^3)$	0.02 (Σ_b)	0.10 (Σ_b)	0.02 (Σ_c)	0.10 (Σ_c)
α_0	0.830	0.823	0.583	0.597
width	0.763 \sim 0.923	0.740 \sim 0.889	0.430 \sim 0.707	0.383 \sim 0.730
f	0.809	0.814	0.527	0.523

Table 4: Values of α_0 , widths, and f for Ξ_b and Ξ_c in the heavy quark limit

$m_D=1.10\text{GeV}$				
$\kappa(\text{GeV}^3)$	0.02 (Ξ_b)	0.10 (Ξ_b)	0.02 (Ξ_c)	0.10 (Ξ_c)
α_0	0.820	0.817	0.553	0.580
width	0.773 \sim 0.857	0.733 \sim 0.877	0.440 \sim 0.647	0.343 \sim 0.700
f	0.809	0.796	0.520	0.471
$m_D=1.15\text{GeV}$				
$\kappa(\text{GeV}^3)$	0.02 (Ξ_b)	0.10 (Ξ_b)	0.02 (Ξ_c)	0.10 (Ξ_c)
α_0	0.810	0.810	0.533	0.510
width	0.753 \sim 0.850	0.717 \sim 0.875	0.393 \sim 0.643	0.300 \sim 0.690
f	0.795	0.791	0.485	0.440
$m_D=1.20\text{GeV}$				
$\kappa(\text{GeV}^3)$	0.02 (Ξ_b)	0.10 (Ξ_b)	0.02 (Ξ_c)	0.10 (Ξ_c)
α_0	0.803	0.803	0.513	0.503
width	0.737 \sim 0.853	0.700 \sim 0.870	0.347 \sim 0.640	0.257 \sim 0.677
f	0.782	0.780	0.445	0.412

Table 5: Values of α_0 , widths, and f for Ω_b and Ω_c in the heavy quark limit

$m_D=1.15\text{GeV}$				
$\kappa(\text{GeV}^3)$	0.02 (Ω_b)	0.10 (Ω_b)	0.03 (Ω_c)	0.10 (Ω_c)
α_0	0.813	0.813	0.573	0.580
width	0.760 \sim 0.853	0.727 \sim 0.873	0.453 \sim 0.667	0.373 \sim 0.710
f	0.802	0.772	0.537	0.460
$m_D=1.20\text{GeV}$				
$\kappa(\text{GeV}^3)$	0.02 (Ω_b)	0.10 (Ω_b)	0.02 (Ω_c)	0.10 (Ω_c)
α_0	0.803	0.810	0.553	0.557
width	0.750 \sim 0.894	0.710 \sim 0.867	0.430 \sim 0.650	0.343 \sim 0.697
f	0.786	0.774	0.510	0.464
$m_D=1.25\text{GeV}$				
$\kappa(\text{GeV}^3)$	0.02 (Ω_b)	0.10 (Ω_b)	0.02 (Ω_c)	0.10 (Ω_c)
α_0	0.797	0.797	0.533	0.540
width	0.733 \sim 0.847	0.697 \sim 0.863	0.393 \sim 0.650	0.313 \sim 0.687
f	0.773	0.770	0.474	0.449

Now we compare the present results with another phenomenological model. In Ref. [10], also based on the quark-diquark picture, Λ_Q is regarded as composed of a heavy quark and a scalar light diquark. The heavy baryon wave function $\Psi_{\Lambda_Q}(\alpha, \mathbf{k}_\perp)$ is proposed as a generalization of the Bauer-Stech-Wirbel [18] meson wave function to the quark-diquark case,

$$\Psi_{\Lambda_Q}(x_1, \mathbf{k}_\perp) = N_{\Lambda_Q} \alpha(1 - \alpha)^3 \exp\{-b^2[\mathbf{k}_\perp^2 + m_{\Lambda_Q}^2(\alpha - \bar{\alpha})^2]\}, \quad (35)$$

where N_{Λ_Q} is the normalization constant, $\bar{\alpha} = m_Q/m_{\Lambda_Q}$, \mathbf{k}_\perp is the transverse momentum and the parameter b is related to the root of the average square of \mathbf{k}_\perp , $\sqrt{\langle \mathbf{k}_\perp^2 \rangle}$. The normalization of the wave function is

$$\int d\alpha d^2\mathbf{k}_\perp |\Psi_{\Lambda_Q}(\alpha, \mathbf{k}_\perp)|^2 = 1. \quad (36)$$

The heavy quark distribution function in this model is defined in the following

$$Q(\alpha) = \int d^2\mathbf{k}_\perp |\Psi_{\Lambda_Q}(\alpha, \mathbf{k}_\perp)|^2, \quad (37)$$

which leads to

$$Q(\alpha) = \frac{2\pi^2 N_{\Lambda_Q}^2}{b^2} \alpha^2 (1 - \alpha)^6 \exp[-2b^2 m_{\Lambda_Q}^2 (\alpha - \bar{\alpha})^2]. \quad (38)$$

Here $\langle \mathbf{k}_\perp^2 \rangle$ is defined as

$$\langle \mathbf{k}_\perp^2 \rangle = \int d\alpha d^2\mathbf{k}_\perp \mathbf{k}_\perp^2 |\Psi_{\Lambda_Q}(\alpha, \mathbf{k}_\perp)|^2, \quad (39)$$

from which, using Eq. (36), we have

$$2b^2 \langle \mathbf{k}_\perp^2 \rangle = 1. \quad (40)$$

We choose $\sqrt{\langle \mathbf{k}_\perp^2 \rangle}$ to vary between 400MeV and 600MeV. For these two parameters we plot $Q(\alpha)$ at the hadronic scale in Fig.6(a) and we plot $\alpha Q(\alpha)$ at $\nu^2 = 10\text{GeV}^2$ in Fig.6(b). We can see from these plots that the heavy quark distribution functions in this model have a similar shape to those found in the present B-S

Table 6: Values of α_0 , widths, and f for Λ_b and Λ_c in the model of Ref. [10]

$\sqrt{\langle \mathbf{k}_\perp^2 \rangle}(\text{GeV})$	0.4 (Λ_b)	0.6 (Λ_b)	0.4 (Λ_c)	0.6 (Λ_c)
α_0	0.816	0.764	0.545	0.460
width	0.766 \sim 0.864	0.693 \sim 0.830	0.426 \sim 0.660	0.306 \sim 0.609
f	0.813	0.758	0.540	0.456

model. The peak position for $Q(\alpha)$, widths of the distributions, and the total “plus” momentum fraction carried by the heavy quark Q , are listed in Table 6. Notice that these values are independent of the value of m_D in this model. Finally, it can be seen from Table 6 that both α_0 and f in this model are smaller than those in the B-S model.

IV. Summary and discussion

Based on our heavy quark and light diquark model for heavy baryons Λ_Q and ω_Q in the B-S equation approach, we have calculated the heavy quark distribution functions in these baryons. This was done in the heavy quark limit for both Λ_Q and ω_Q . Furthermore, $1/m_Q$ corrections were also included in the case of Λ_Q . Our numerical results show that for different heavy baryons with the same heavy quark flavor the shapes of the heavy quark distribution functions are similar. At the hadronic scale, Λ_{QCD} , they have an obvious peak at some “plus” momentum fraction carried by the heavy quark, α_0 , which is much closer to 1 for b -baryons than c -baryons. In addition, the widths of these distributions are much smaller for b -baryons than c -baryons. Furthermore, we have found that the peaks of the heavy quark distribution functions become lower and their widths bigger when the confinement between the heavy quark and light diquark inside a heavy baryon is stronger. The QCD evolution of these distribution functions were also discussed by applying DGLAP equations to the next-to-leading order and the results show that

the distinction between b -quark and c -quark distribution functions is still obvious at high ν^2 . The evolution makes the amplitudes of the peaks much smaller, especially for the distribution functions in b -baryons. We also calculated the total “plus” momentum fraction carried by the heavy quark, which is much bigger for b -baryons than c -baryons. The dependence of all these numerical results on the parameters in our model was discussed in detail. We also checked the normalization condition of these distribution functions and found that it is satisfied. In addition, we compared our results with an existing phenomenological model for Λ_Q proposed in Ref. [10]. It was found that the shapes of the heavy quark distribution functions in these two models are quite similar, although the peak positions in the B-S model are closer to 1 than those in the model of Ref. [10]. We also compared our results for the heavy quark distribution functions with the general argument of Close and Thomas based on energy and momentum conservation. It was found that the peak positions of the quark distribution functions move closer to 1 and the peak values become bigger when the quark masses increase.

Although we cannot determine the exact value of ν_0 , the hadronic scale at which the heavy quark distribution functions are calculated, our results do reflect nonperturbative information in the heavy baryons Λ_Q and ω_Q . We have treated ν_0 as a parameter to be determined by experiment. Even though the heavy quark distribution functions cannot be measured directly from deep inelastic scattering processes, we can still expect to obtain some information about these functions from the decays of heavy baryons and fragmentation of heavy quarks to heavy baryons. In fact, the latter is directly related to experimental measurements of fragmentation processes. However, the theoretical extension to address fragmentation processes is more complicated. This is currently under investigation.

Acknowledgment:

One of us (Guo) gratefully acknowledges F.-G. Cao for helpful discussions. He also thanks O. Leitner and F. Bissey for assistance in preparing the figures. This work was supported by the Australian Research Council.

References

- [1] C. Boros and A.W. Thomas, Phys.Rev. **D60** (1999) 074017.
- [2] N. Isgur and M.B. Wise, Phys. Lett. **B232** (1989) 113, **B237** (1990) 527; H. Georgi, Phys. Lett. **B264** (1991) 447; see also M. Neubert, Phys. Rep. **245** (1994) 259 for the review.
- [3] OPAL collaboration, R. Akers et al., Z. Phys. **C69** (1996) 195; Phys. Lett. **B353** (1995) 402; OPAL collaboration, K. Ackerstaff et al., Phys. Lett. **B426** (1998) 161.
- [4] UA1 Collaboration, C. Albarjar et al., Phys. Lett. **B273** (1991) 540.
- [5] CDF Collaboration, F. Abe et al., Phys.Rev. **D47** (1993) 2639.
- [6] S.E. Tzmarias, invited talk presented in the 27th International Conference on High Energy Physics, Glasgow, July 20-27, 1994; P. Abreu et al., Phys. Lett. **B374** (1996) 351.
- [7] V.N. Gribov and L.N. Lipatov, Sov. J. Nucl. Phys. **15** (1972) 438; **15** (1972) 675; G. Altarelli and G. Parisi, Nucl. Phys. **B126** (1977) 298; Yu.L. Dokshitzer, Zh. Eksp. Teor. Fiz. **73** (1977) 1216 [Sov. Phys. JETP **46** (1977) 641].
- [8] M. Göckeler *et al.*, Phys. Rev. **D53** (1996) 2317; M. Göckeler *et al.*, Nucl. Phys. Proc. Suppl. **53** (1997) 81; D. Dolgov *et al.*, Nucl. Phys. Proc. Suppl. **94** (2001) 303; D. Dolgov, Ph.D. thesis, MIT, Sep. 2000; W. Detmold, W. Melnitchouk, J.W. Negele, D.B. Renner and A.W. Thomas, hep-lat/0103006.
- [9] X.-H. Guo and T. Muta, Phys. Rev. **D54** (1996) 4629, Mod. Phys. Lett. **A11** (1996) 1523; X.-H. Guo, A.W. Thomas and A.G. Williams, Phys. Rev. **D59** (1999) 116007, Phys. Rev. **D61** (2000) 116015.
- [10] X.-H. Guo and P. Kroll, Z. Phys. **C59** (1993) 567.
- [11] J.C. Collins and D.E. Soper, Nucl. Phys. **B194** (1982) 445.
- [12] R.L. Jaffe, Nucl. Phys. **B229** (1983) 205.

- [13] M. Miyama and S. Kumano, *Comput. Phys. Commun.* **94** (1996)185.
- [14] M. Anselmino, P. Kroll and B. Pire, *Z. Phys.* **C36** (1987) 89; P. Kroll, B. Quadder and W. Schweiger, *Nucl. Phys.* **B316** (1988) 373.
- [15] E. Eichten, K. Gottfried, T. Kinoshita, K.D. Lane and T.-M. Yan, *Phys. Rev.* **D17** (1978) 3090.
- [16] H.-Y. Jin, C.-S. Huang and Y.-B. Dai, *Z. Phys.* **C56** (1992) 707; Y.-B. Dai, C.-S. Huang and H.-Y. Jin, *Z. Phys.* **C60** (1993) 527; Y.-B. Dai, C.-S. Huang and H.-Y. Jin, *Z. Phys.* **C65** (1995) 87.
- [17] F. Close and A.W. Thomas, *Phys. Lett.* **B212** (1988) 227.
- [18] M. Wirbel, B. Stech and M. Bauer, *Z. Phys.* **C29** (1985) 637; M.Bauer, B.Stech and M.Wirbel, *Z. Phys.* **C34** (1987) 103.

Figure Captions

Fig.1 (a) Heavy quark distribution functions at the hadronic scale ν_0^2 with the B-S equation solved for Λ_Q in the limit $m_Q \rightarrow \infty$; (b) $\alpha Q(\alpha)$ for Λ_Q at $\nu^2 = 10\text{GeV}^2$ in the limit $m_Q \rightarrow \infty$. The lines on the right (left) are for Λ_b (Λ_c). The solid (dot) lines correspond to $m_D = 0.70\text{GeV}$ and $\kappa = 0.02\text{GeV}^3$ ($\kappa = 0.10\text{GeV}^3$). The dashed (dot dashed) lines correspond to $\kappa = 0.06\text{GeV}^3$ and $m_D = 0.65\text{GeV}$ ($m_D = 0.75\text{GeV}$).

Fig.2 (a) Heavy quark distribution functions at the hadronic scale ν_0^2 with the B-S equation solved for Λ_Q to order $1/m_Q$; (b) $\alpha Q(\alpha)$ for Λ_Q at $\nu^2 = 10\text{GeV}^2$ to order $1/m_Q$. The lines on the right (left) are for Λ_b (Λ_c). The solid (dot) lines correspond to $m_D = 0.70\text{GeV}$ and $\kappa = 0.02\text{GeV}^3$ ($\kappa = 0.10\text{GeV}^3$). The dashed (dot dashed) lines correspond to $\kappa = 0.06\text{GeV}^3$ and $m_D = 0.65\text{GeV}$ ($m_D = 0.75\text{GeV}$).

Fig.3 (a) Heavy quark distribution functions at the hadronic scale ν_0^2 with the B-S equation solved for Σ_Q in the limit $m_Q \rightarrow \infty$; (b) $\alpha Q(\alpha)$ for Σ_Q at $\nu^2 = 10\text{GeV}^2$ in the limit $m_Q \rightarrow \infty$. The lines on the right (left) are for Σ_b (Σ_c). The solid (dot) lines correspond to $m_D = 0.95\text{GeV}$ and $\kappa = 0.02\text{GeV}^3$ ($\kappa = 0.10\text{GeV}^3$). The dashed (dot dashed) lines correspond to $\kappa = 0.06\text{GeV}^3$ and $m_D = 0.90\text{GeV}$ ($m_D = 1.00\text{GeV}$).

Fig.4 (a) Heavy quark distribution functions at the hadronic scale ν_0^2 with the B-S equation solved for Ξ_Q in the limit $m_Q \rightarrow \infty$; (b) $\alpha Q(\alpha)$ for Ξ_Q at $\nu^2 = 10\text{GeV}^2$ in the limit $m_Q \rightarrow \infty$. The lines on the right (left) are for Ξ_b (Ξ_c). The solid (dot) lines correspond to $m_D = 1.15\text{GeV}$ and $\kappa = 0.02\text{GeV}^3$ ($\kappa = 0.10\text{GeV}^3$). The dashed (dot dashed) lines correspond to $\kappa = 0.06\text{GeV}^3$ and $m_D = 1.10\text{GeV}$ ($m_D = 1.20\text{GeV}$).

Fig.5 (a) Heavy quark distribution functions at the hadronic scale ν_0^2 with the B-S equation solved for Ω_Q in the limit $m_Q \rightarrow \infty$; (b) $\alpha Q(\alpha)$ for Ω_Q at $\nu^2 = 10\text{GeV}^2$ in the limit $m_Q \rightarrow \infty$. The lines on the right (left) are for Ω_b (Ω_c). The solid (dot) lines correspond to $m_D = 1.20\text{GeV}$ and $\kappa = 0.02\text{GeV}^3$ ($\kappa = 0.10\text{GeV}^3$). The dashed (dot dashed) lines correspond to $\kappa = 0.06\text{GeV}^3$ and $m_D = 1.15\text{GeV}$ ($m_D = 1.25\text{GeV}$).

Fig.6 (a) Heavy quark distribution functions for Λ_Q in the model of Ref. [10]; (b) $\alpha Q(\alpha)$ for Λ_Q at $\nu^2 = 10\text{GeV}^2$ in the model of Ref. [10]. The two lines on the right (left) are for Λ_b (Λ_c). The solid (dashed) lines correspond to $\sqrt{\langle k_\perp \rangle^2} = 0.4\text{GeV}$ ($\sqrt{\langle k_\perp \rangle^2} = 0.6\text{GeV}$).

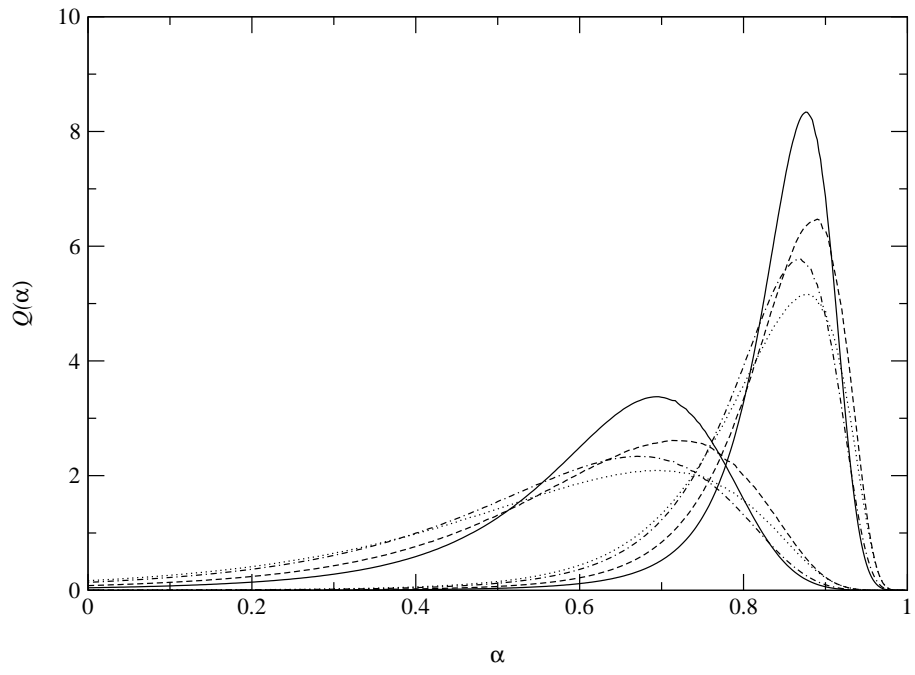


Fig.1(a)

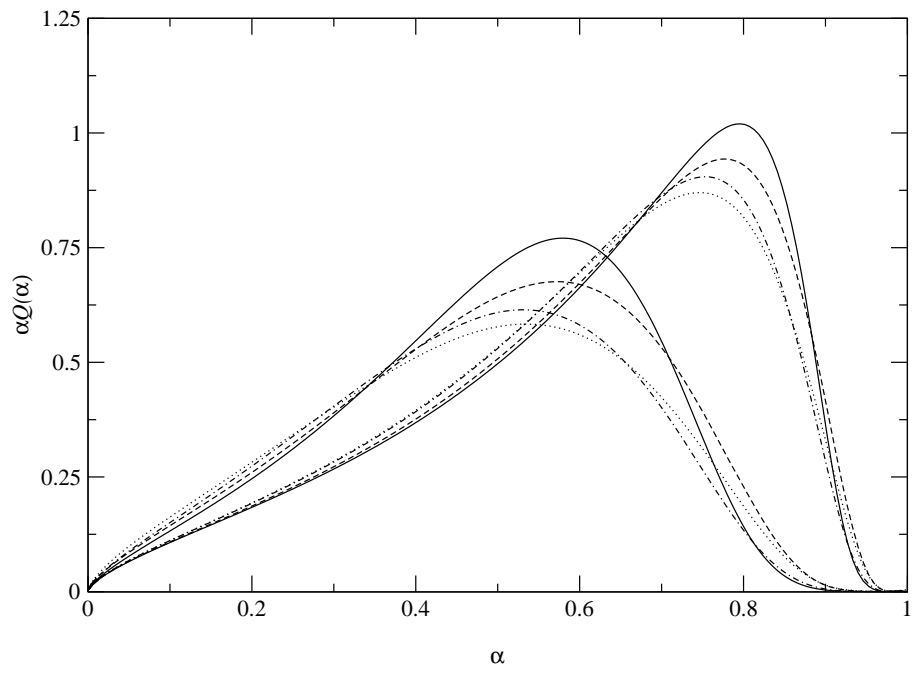


Fig.1(b)

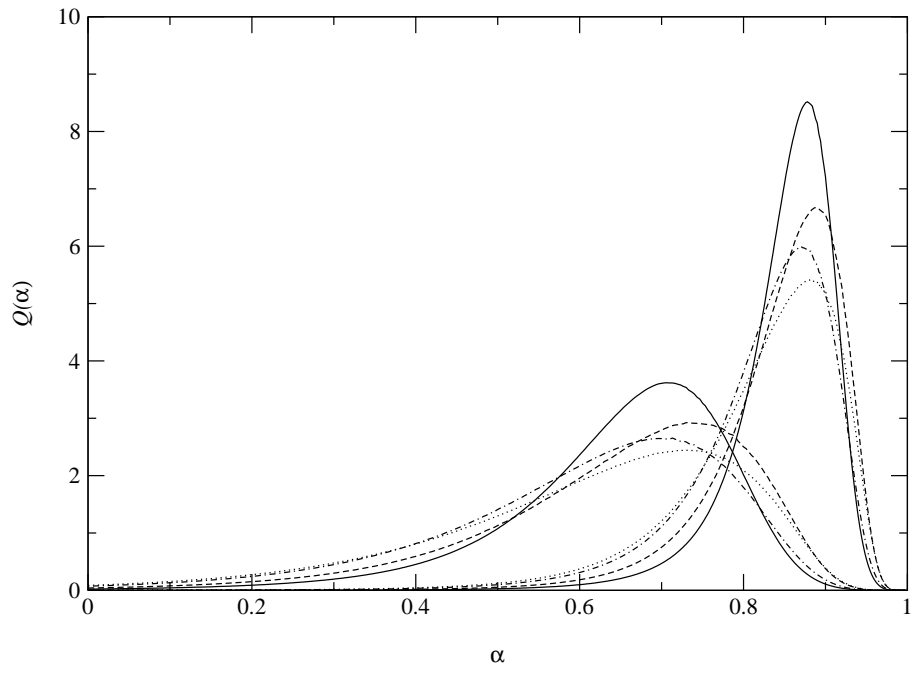


Fig.2(a)

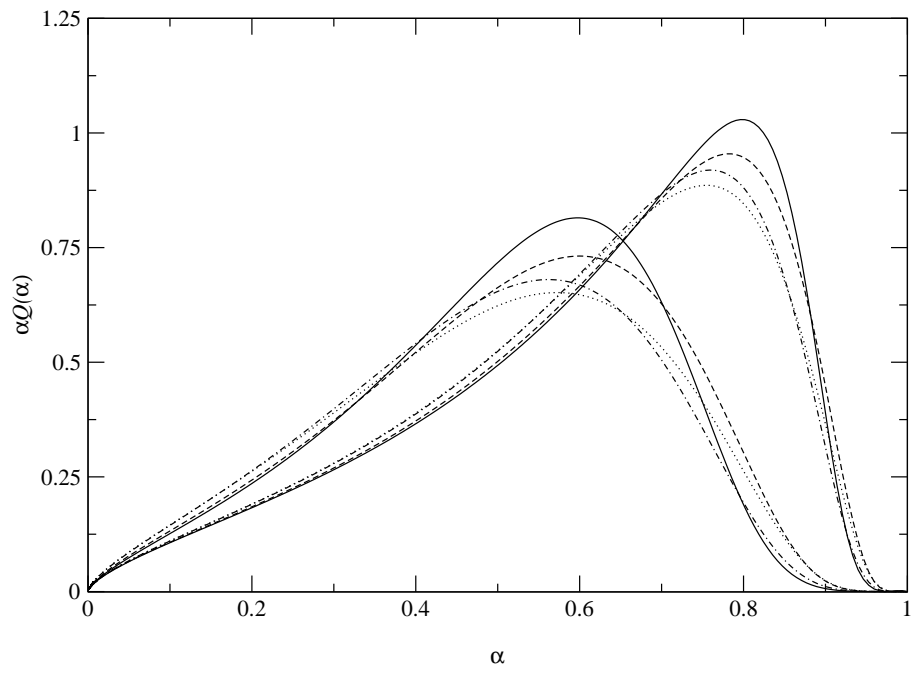


Fig.2(b)

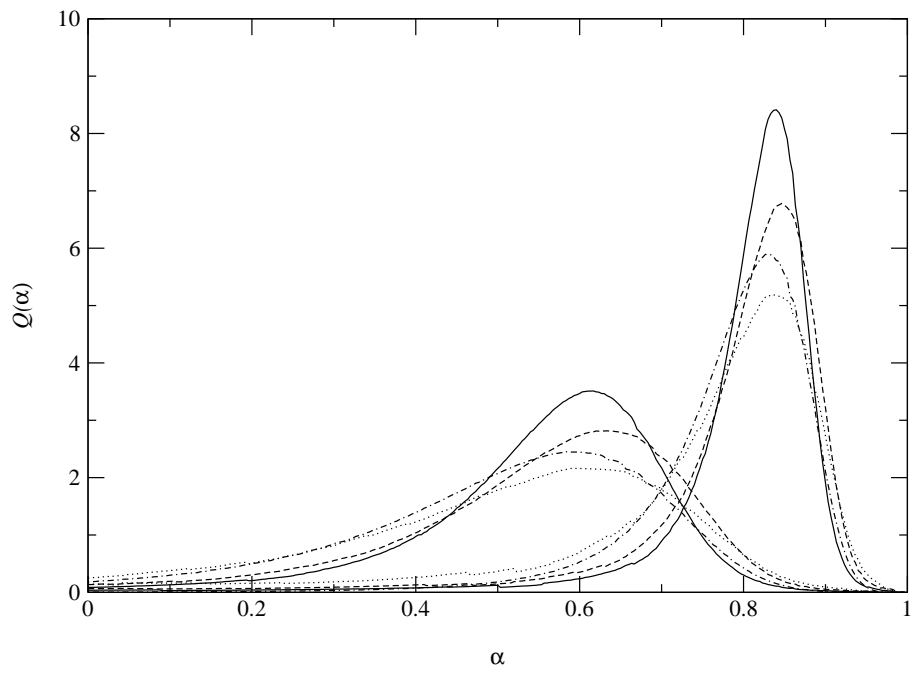


Fig.3(a)

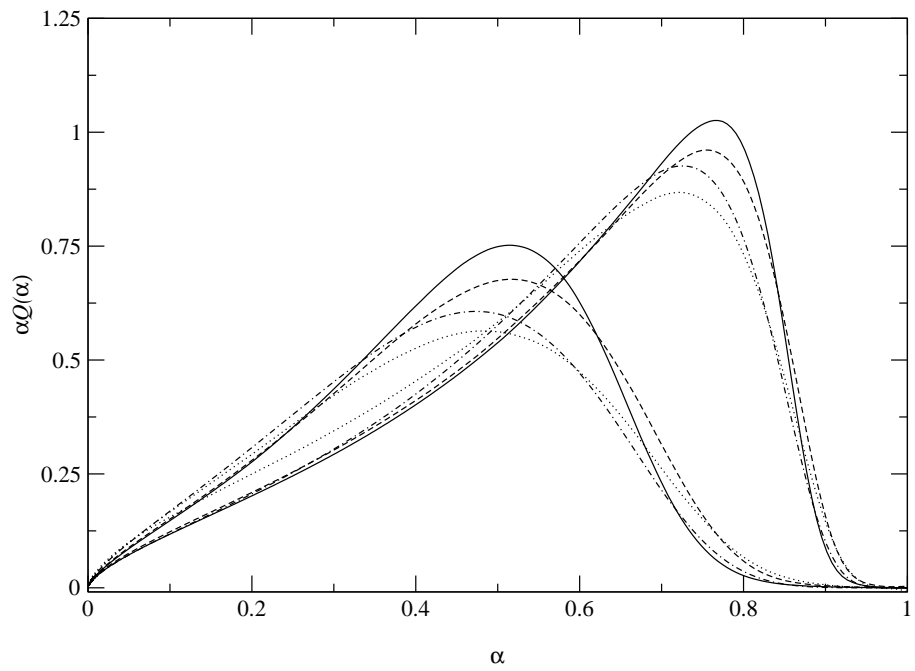


Fig.3(b)

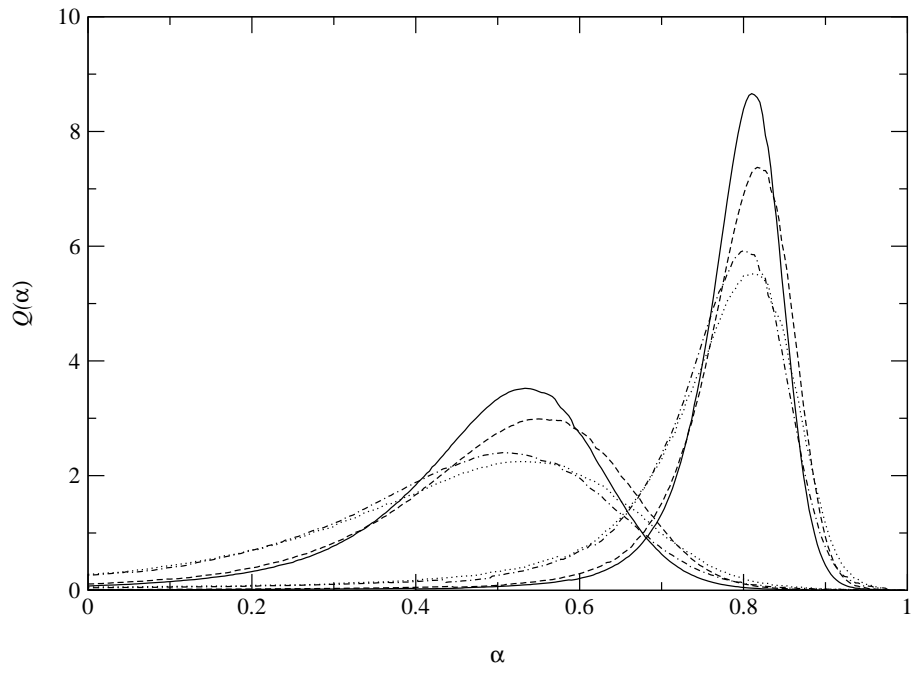


Fig.4(a)

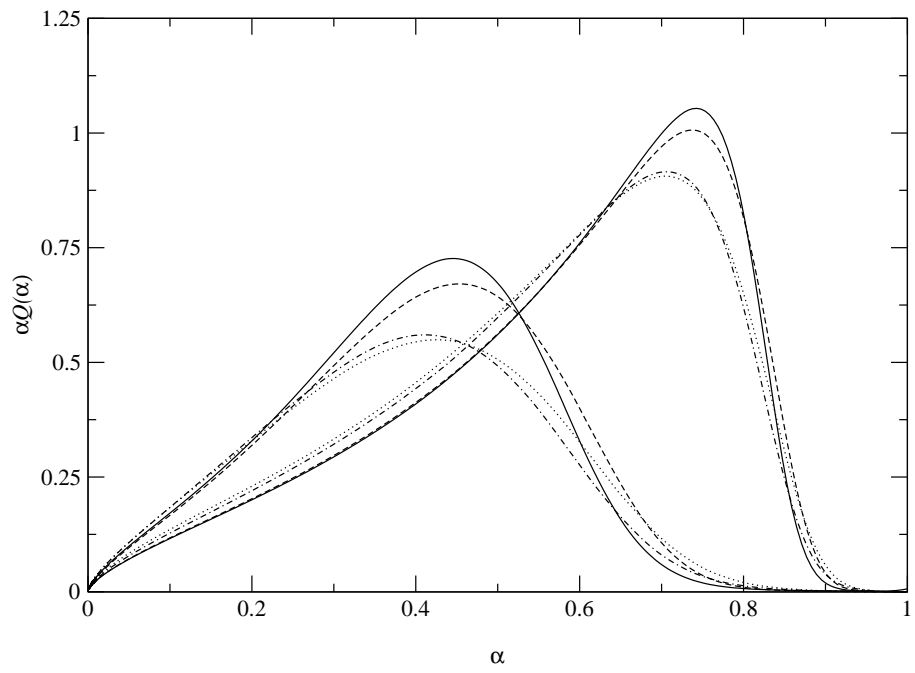


Fig.4(b)

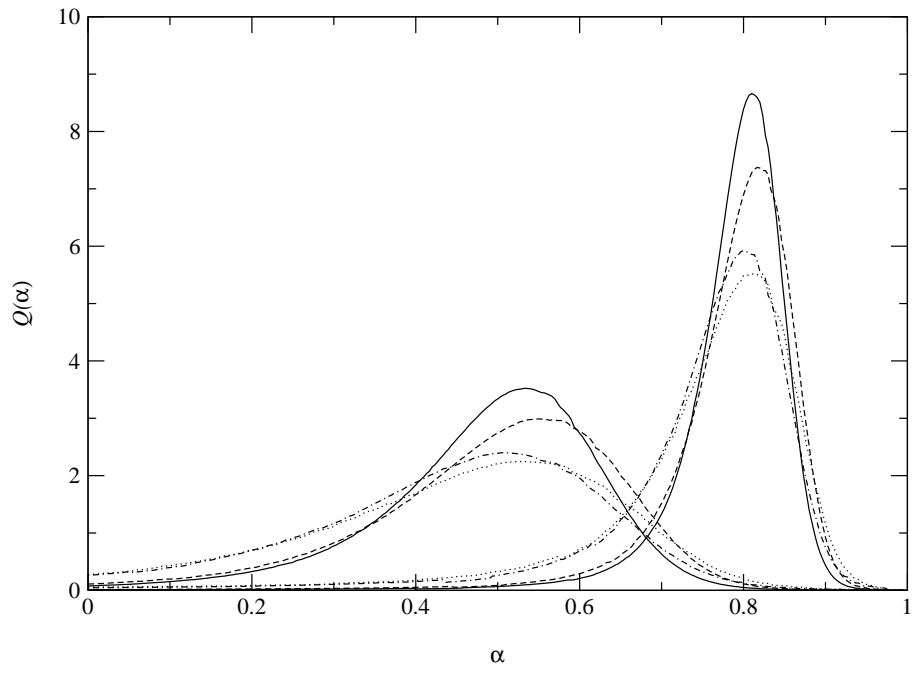


Fig.5(a)

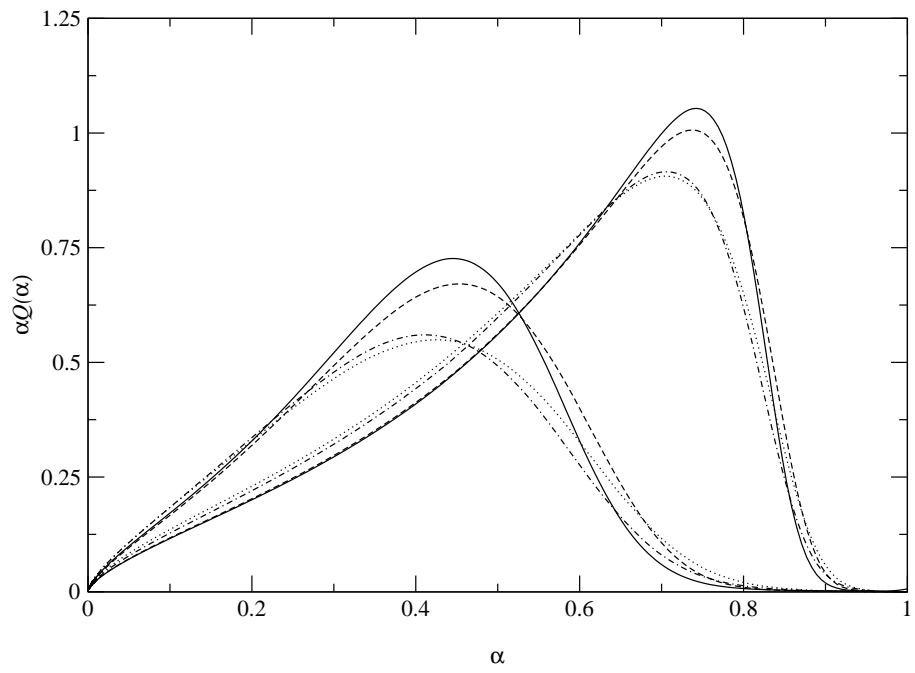


Fig.5(b)

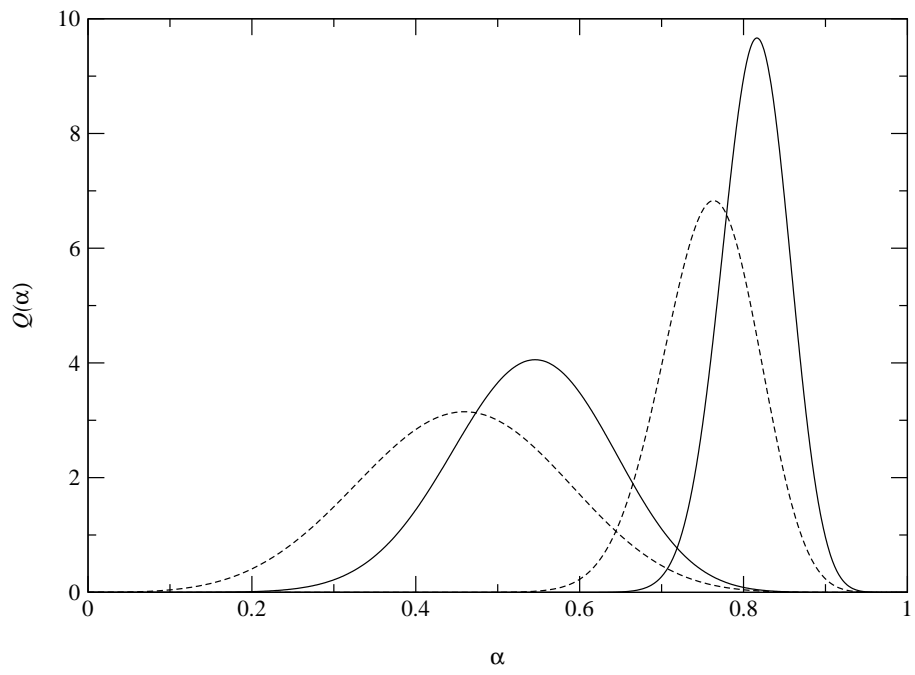


Fig.6(a)

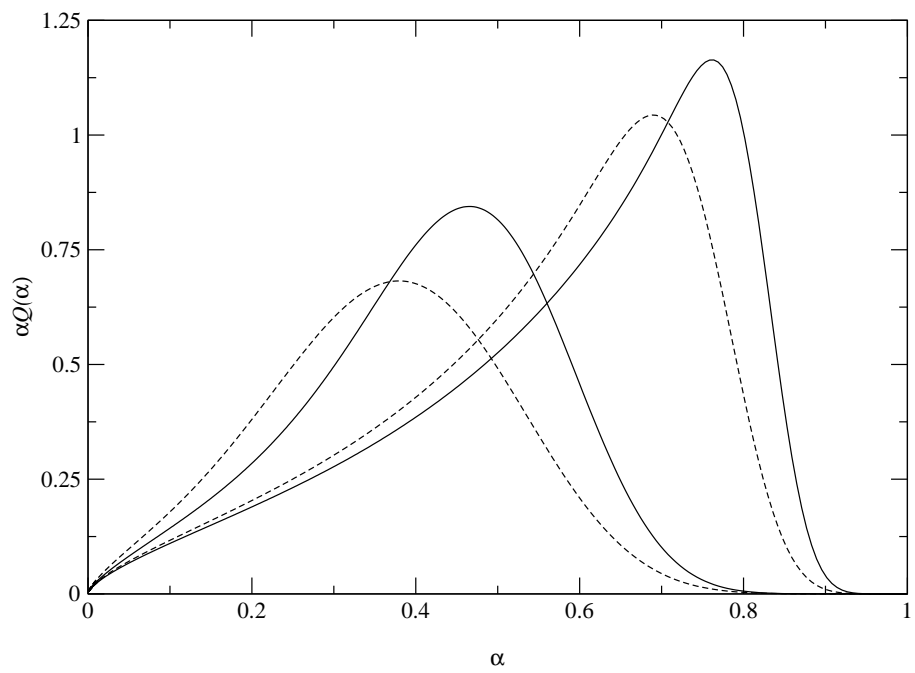


Fig.6(b)